*Korean J. Chem. Eng.*, 39(6), 1576-1587 (2022)
DOI: 10.1007/s11814-022-1072-9

pISSN: 0256-1115
eISSN: 1975-7220

# Application of PC-SAFT EoS for calculating gas solubility and viscosity of ammonium-based ionic liquids

**Alireza Afsharpour† and Seyyed Hamid Esmaeli-Faraj**

Faculty of Chemical and Materials Engineering, Shahrood University of Technology, Shahrood, Iran
(*Received 17 August 2021 • Revised 5 January 2022 • Accepted 19 January 2022*)

**Abstract**−The well-known perturbed-chain-statistical-association-fluid-theory (PC-SAFT) EoS was employed to model $CO_2$ and $H_2S$ absorption in some protic ammonium-based ionic liquids, including Methyl-diethanol-ammonium Formate, Methyl-diethanol-ammonium Acetate, Dimethyl-ethanol-ammonium Formate, and Dimethyl-ethanol-ammonium Acetate. In this way, all the acidic gases and the ILs were considered as associative compounds so that they can establish hydrogen bonding by their own or other molecules. Accordingly, 4C, 2B, and 1A association schemes were assumed for $H_2S$, the ILs, and $CO_2$, respectively. Moreover, to estimate the liquid phase concentrations, a complex formation reaction (CFR) approach was followed. In this concept, acidic gases are supposed to form chemical complexes with the ILs. To show the importance of the reactions, the solubilities were calculated with and without using them, and the achieved results were compared. As the outputs show, considering the reactions, the excellent overall AADs% equal to 1.38 and 0.17 were obtained for $H_2S$ and $CO_2$ absorption, respectively. While without them, these values were about 5.05 and 8.57. In the second part of the work, the viscosity of the used ILs was estimated through a new approach that combines the free-volume-theory (FVT) and the PC-SAFT, CPA, and mSRK EoSs. Accordingly, the density of the ILs computed using the EoSs, and then FVT was applied to estimate the dynamic viscosity. Based on the outputs, all the EoSs illustrate good ability to calculate viscosities, precisely, so that all the models present AAD% of about 2.5. This is because of the high ability of the FVT to obtain a precise estimation of viscosity using a rough estimation of the density.

Keywords: PC-SAFT, EoS, Viscosity, CFR, FVT, CPA

## INTRODUCTION

The tunability of the Ionic Liquids (ILs) makes them good candidates for various applications. Indeed, it is possible to arrive at the desired characteristics by choosing suitable cations and anions. One of the ongoing uses of the ILs is to employ them as solvents or cosolvents of acidic gases [1]. A specific category of such compounds, known as Protic ILs (PILs) are able to form hydrogen bonding with the acidic gases and therefore can dissolve them. It is for the sake of their potential to release at least one proton [2]. This potency, along with the insignificant volatility, thermodynamical and electrochemical stability and etcetera, are the main reasons to select these materials.

Despite the mentioned advantages, up to now, limited experimental studies have been done on the absorption of acidic gases by the ILs. It is because of the time, cost, and energy-consuming essence of such experiments. Thus, a theoretical study based on rigorous models could be noticed [3].

So far, many thermodynamical models from different categories have been proposed and investigated for these systems. Recently, among the existing models, SAFT variants have been noticed because of their accuracies [4]. A few such works are reviewed here.

Al-Fnaish and Lue [5] employed PC-SAFT EoS to model absorption of $CO_2$ and $H_2S$ in [$C_{2\text{-}8}$ mim][$Tf_2N$] ionic liquids. The pure parameters were found by using ILs density data. Moreover, solubility data were used to find binary interaction parameters. According to the results, overall ARD% below 7 and 5 were obtained for $H_2S$ and $CO_2$, respectively.

EPC-SAFT EoS was implemented to investigate gas solubility in some ILs with [$BF_4$], [$PF_6$], and [$Tf_2N$] anions by Ji et al. [6]. The Debye-Hückel theory was also utilized to take the long-range interactions into account. In a similar survey [7], they also applied the same EoS to correlate hydrogen sulfide absorption in some imidazolium-based ILs with acceptable deviations.

SAFT-VR EoS was used to calculate phase equilibria in $CO_2$ removal using aqueous alkylamine solutions in the work of MacDowel et al. [8]. In all the studied systems, AADs% below 4 are observed.

Zhu et al. [9] presented two machine learning approaches including artificial neural networks and eXtreme gradient boosting to assist filtered two-fluid model to predict multiphase flows.

Xiong et al. [10] utilized four super-basic ILs as solvents for $CO_2$/$H_2S$ removal from methane. Physical properties of the ILs were measured. Moreover, the 'deactivated model' was implemented to estimate thermodynamic parameters such as enthalpy and entropy. In another work [11], they designed some TSILs to absorb and convert $H_2S$ to useful mercaptan acids.

On the other hand, physical properties estimation using a precise

†To whom correspondence should be addressed.
E-mail: A.Afsharpour@Shahroodut.ac.ir

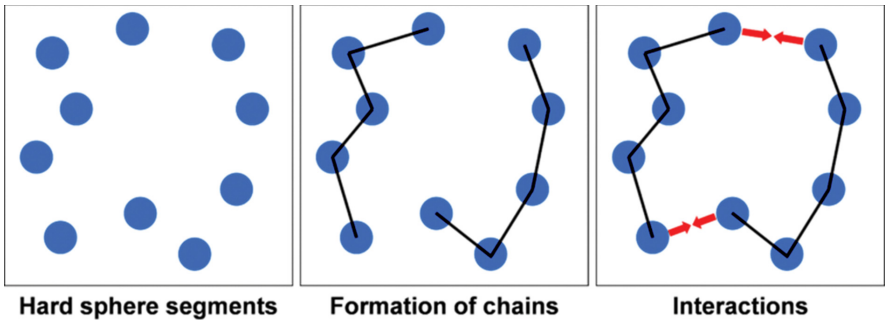


**Fig. 1. Chain dispersion concept in the PC-SAFT EoS: Segment attractions- Chain formation- Association formation.**

model is another challenge in the way of modeling processes. One of these properties is the dynamic viscosity as a transport property. There exist some approaches to estimating the dynamic viscosity by using thermodynamic models. One of them is to use of free-volume-theory (FVT). Some works on FVT are mentioned here.

Llovell et al. [12] combined FVT and Soft-SAFT EoS to obtain the viscosity of Lennard-Jones (LJ) fluids. They investigated a large family of n-alkanes and compared the results with those of molecular simulation data. Good agreement between both of results was seen so that AADs were calculated under 4%.

The viscosity of petroleum fluids was predicted using FVT+PCSAFT by Khoshnamvand & Assareh [13]. They studied twenty-two real samples with °API between 22 to 45. The overall AAD% equal to 9.7 was achieved.

In the work of Shen et al. [14], FVT was combined with the ePC-SAFT to model the viscosity of ILs. In this work, 12 adjustable parameters were utilized and good results were obtained.

Considering good results of the FVT model and the PC-SAFT EoS, in the present research, the solubility of solitary acidic gases (including $CO_2$ and $H_2S$) in four ammonium-based PILs including Methyl-diethanol-ammonium Formate ([MDEAH][For]), Methyl-diethanol-ammonium Acetate ([MDEAH][Ac]), Dimethyl-ethanol-ammonium Formate ([DMEAH][For]) and Dimethyl-ethanol-ammonium Acetate ([DMEAH][Ac]) was simulated applying PC-SAFT EoS with and without employing complex formation reaction (CFR) approach. In addition, the dynamic viscosity of the pure ILs was predicted through a new approach combining FVT and PC-SAFT/CPA/mSRK EoS.

## THERMODYNAMIC MODELING

### 1. Complex Formation Reactions (CFR)

The formation of some complexes between acid gas and IL was first proposed by Huang et al. [15] to describe the absorption process through a chemical reaction-like mechanism. As shown in [2], the possibility of the first reaction is almost zero for the investigated system. Therefore:

$$\{CO_2/H_2S\}(g)+2[Ca][An](1)\xrightarrow{K}\{CO_2/H_2S\}([Ca][An])_2 \quad (1)$$

in which Ca, An, stand for the cations and anions, respectively.

Therefore, equilibrium constant relations together with Henry's law and mass balance equations could be combined and simplified as the below relation [15]:

$$\hat{n}_{AG_0}=\frac{\hat{n}_{IL_0}}{2}+\frac{P}{H}+\frac{[1-\sqrt{8KP\hat{n}_{IL_0}+1}]}{8KP} \quad (2)$$

where $\hat{n}_{AG_0}$ and $\hat{n}_{IL_0}$ represent the initial molality of the acidic gas and the IL, respectively.

Parameters K (equilibrium constants of the complex formation reaction) and H (Henry's law constant) were taken from the previous work [2].

After computing the liquid phase mole fractions, VLE calculations will be the next step.

More descriptive details about the CFR can be found in [15].

### 2. Perturbed Chain SAFT (PC-SAFT) Equation of State

The PC-SAFT was introduced by Gross and Sadowski as an SAFT variant EoS [16]. The main difference between this model and other variants of SAFT EoS returns to the implemented dispersion term. This term tries to take the dispersion attraction between whole chains into account. A conceptual molecular model of PC-SAFT EoS is presented in Fig. 1.

The PC-SAFT can be presented on the basis of reduced residual Helmholtz energy as Eq. (3):

$$\tilde{a}^{res}=\tilde{a}^{hc}+\tilde{a}^{disp}+\tilde{a}^{assoc.} \quad (3)$$

where $\tilde{a}^{hc}$, $\tilde{a}^{disp}$, and $\tilde{a}^{assoc.}$ denote reduced Helmholtz energy of the hard chain, dispersion, and the association terms, respectively. According to the PC-SAFT variation, the mentioned terms could be defined as below.

2-1. Hard Chain Term

Based on Chapman et al's EoS [17,18], the reduced Helmholtz energy of the hard chain term is as below:

$$\tilde{a}^{hc}=m\tilde{a}^{hs}-\sum_i x_i(m_i-1)\ln g_{ii}^{hs}(\sigma_{ii}) \quad (4)$$

where m, $\tilde{a}^{hs}$, $g_{ii}^{hs}(\sigma_{ii})$ stand for segment number, hard-sphere reduced Helmholtz energy and radial distribution function [19], respectively. The mentioned parameters are defined as:

$$m=\sum_i x_i m_i \quad (5)$$

$$\tilde{a}^{hs}=\frac{1}{\xi_0}\left[\frac{3\xi_1\xi_2}{(1-\xi_3)}+\frac{\xi_2^3}{\xi_3(1-\xi_3)^2}-\left(\xi_0-\frac{\xi_2^3}{\xi_3^2}\right)\right]\ln(1-\xi_3) \quad (6)$$

$$g_{ij}^{hs}=\frac{1}{1-\xi_3}+\left(\frac{d_i d_j}{d_i+d_j}\right)\frac{3\xi_2}{(1-\xi_3)^2}+\left(\frac{d_i d_j}{d_i+d_j}\right)^2\frac{2\xi_2^2}{(1-\xi_3)^3} \quad (7)$$

that

$$\xi_k=\left(\frac{\pi}{6}\rho\right)\sum x_i m_i d_i^k \quad n\in\{0,1,2,3\} \tag{8}$$

$$d_i=\sigma_i\left[1-0.12\exp\left(-3\frac{\varepsilon_i}{kT}\right)\right] \tag{9}$$

$\sigma_i$, $\varepsilon_i$/k and $\rho$ represent segment diameter, segment energy and density, respectively.

2-2. Dispersion Term

The reduced Helmholtz energy of the dispersion term is as below [16,20]:

$$\tilde{a}^{disp}=(-2\pi\rho I_1\overline{m^2\sigma^3})+(-\pi\rho m C_1 I_2\overline{m^2\varepsilon^2\sigma^3}) \tag{10}$$

in which

$$\overline{m^2\sigma^3}=\Sigma_i\Sigma_j x_i x_j m_i m_j\left(\frac{\varepsilon_{ij}}{kT}\right)\sigma_{ij}^3 \tag{11}$$

$$\overline{m^2\varepsilon^2\sigma^3}=\Sigma_i\Sigma_j x_i x_j m_i m_j\left(\frac{\varepsilon_{ij}}{kT}\right)^2\sigma_{ij}^3 \tag{12}$$

$$C_1=\left(1+m\frac{8\xi_3-2\xi_3^2}{(1-\xi_3)^4}+(1-m)\frac{20\xi_3-27\xi_3^2+12\xi_3^3-2\xi_3^4}{[(1-\xi_3)(2-\xi_3)]^2}\right)^{-1} \tag{13}$$

$$I_1(\xi_3,m)=\sum_{i=0}^{6}a_i(m)\xi_3^i \tag{14}$$

$$I_2(\xi_3,m)=\sum_{i=0}^{6}b_i(m)\xi_3^i \tag{15}$$

So that

$$\sigma_{ij}=\frac{1}{2}(\sigma_i+\sigma_j) \tag{16}$$

$$\varepsilon_{ij}=\sqrt{\epsilon\varepsilon_{ii}\epsilon\varepsilon_{jj}}(1-k_{ij}) \tag{17}$$

$$a_i(m)=a_{0i}+\frac{m-1}{m}a_{1i}+\frac{m-1}{m}\frac{m-2}{m}a_{2i} \tag{18}$$

$$b_i(m)=b_{0i}+\frac{m-1}{m}b_{1i}+\frac{m-1}{m}\frac{m-2}{m}b_{2i} \tag{19}$$

The constants $a_{ki}$ and $b_{ki}$ have been reported in the literature [21]. Moreover, $k_{ij}$s are the binary interaction coefficients between i and j species and can be optimized utilizing experimental data.

2-3. Association Term

The Wertheim's association term [22-25] contributes the hydrogen bonging effects as follows:

$$\tilde{a}^{assoc.}=\sum_i x_i\sum_{A_i}\left[\ln X_{A_i}-\frac{1}{2}X_{A_i}+\frac{1}{2}\right] \tag{20}$$

$X_{A_i}$ is the main parameter of the association term. It stands for the A-type site fractions at $i^{th}$ molecule that do not establish hydrogen bonding with the other active sites. It is calculated as

$$X^{A_i}=\frac{1}{1+\rho\sum_j x_j\sum_{B_j}X^{B_j}\Delta^{A_iB_j}} \tag{21}$$

So that the $\Delta^{A_iB_j}$ is interpreted as the association strength and defined as below:

$$\Delta^{A_iB_j}=d_{ij}^3 g_{ij}^{hs}(d_{ij})\kappa^{A_iB_j}\left[\exp\left(\frac{\varepsilon^{AB_j}}{kT}\right)-1\right] \tag{22}$$

where $\varepsilon^{AB}$ and $\kappa^{A_iB_j}$ are known as the energy and volume of the association, respectively.

**3. Modified SRK Equation of States**

A specialized version of the Redlich-Kwong EoS [26] for ILs, by Yokozeki and Schiflett [27], was applied to correlate acid gas solubility in the previous work [2]. In this work, this model will be utilized to estimate the ILs dynamic viscosities. For a pure component we have:

$$P=\frac{RT}{V-b}-\frac{a(T)}{V(V+b)} \tag{23}$$

$$a(T)=0.427480\frac{R^2T_c^2}{P_c}\alpha(T) \tag{24}$$

$$b=0.08664\frac{RT_c}{P_c} \tag{25}$$

So that for ILs

$$\alpha(T)=1+\beta_1\left(\frac{T_c}{T}-\frac{T}{T_c}\right) \tag{26}$$

In which $\beta_1$ belong to the pure ILs and have been taken from [2].

**4. Cubic Plus Association (CPA) Equation of State**

As expected from its name, EoS contains a cubic part and an association one. The classic form of this model was proposed by Kontogeorgis et al. [28] in which cubic part is the SRK EoS and the association term is from Wertheim's theory.

$$\tilde{a}_{CPA}=\tilde{a}_{SRK}+\tilde{a}_{Assoc.} \tag{27}$$

In this way, the association part will be the same presented in section 2.2.3. Moreover, the SRK part could be presented as below:

$$\tilde{a}_{SRK}=\frac{a(T)}{RTb}\ln\left(\frac{v}{v+b}\right)+\ln\left(\frac{v}{v-b}\right) \tag{28}$$

wherein

$$a(T)=a_0[1+c(1-\sqrt{T_r})]^2 \tag{29}$$

Complete details about the model together with the obtained parameters have been presented in the previous works [1,2,29].

**5. Free Volume Theory (FVT)**

Allal et al. [30] introduced their model to estimate dynamic viscosity based on the free volume theory of Cohen and Turnbull [31]. Their proposed model is known as the FVT model. According to the model, the dynamic viscosity ($\eta$) of a dense fluid (e.g., liquids) can be determined through the following relation:

$$\eta=\eta_0+\Delta\eta \tag{30}$$

In which $\eta_0$ is related to the dilute gas viscosity while $\Delta\eta$ is the dense states correction term.

$$\eta_0=4.0785\times10^{-5}\frac{\sqrt{M_wT}}{v_c^{\frac{2}{3}}\Omega^*}(1-0.2756w) \tag{31}$$

$$\Delta\eta=\rho L\frac{\left(E_0+\frac{PM_w}{\rho}\right)}{\sqrt{3RTM_w}}\exp\left(B\left(\frac{E_0+\frac{PM_w}{\rho}}{2RT}\right)^{1.5}\right) \quad (32)$$

So that

$$\Omega^*=\frac{1.16145}{T^{*0.14874}}+\frac{0.52478}{e^{0.7732T^*}}+\frac{2.16178}{e^{2.73787T^*}}-6.43\times10^{-4}T^{*0.14874}\sin(18.0323T^{*-0.76830}-7.27371) \quad (33)$$

wherein

$$T^*=\frac{1.2593T}{T_c} \quad (34)$$

$M_w$, $v_c$, w, $\rho$, and R represent molecular weight, critical volume, acentric factor, density, and the universal gas constant, respectively. Moreover, L, $E_0$ and B are the adjustable parameters of the model and stand for the diffuse barrier energy of the molecule, free space formation parameter and a dimensionless constant, respectively. All the parameters are in the SI system.

More details for FVT are presented in [30].

## RESULTS AND DISCUSSION

### 1. The Pure Component Physical Properties

To implement the FVT model, some physical properties including $T_c$, w and $v_c$ should be determined. As these data do not exist in the literature, the Modified Lydersen-Joback-Reid: mLJR method by Valderrama and Robles [32] was employed. In this way, critical temperature, critical volume and acentric factor can be estimated applying the below relations, respectively.

$$T_b=198.2+\sum n\Delta T_{bM} \quad (35)$$

$$T_c=\frac{T_b}{A_M+B_M\sum n\Delta T_M-(\sum n\Delta T_M)^2} \quad (36)$$

$$P_c=\frac{M}{[C_M+\sum n\Delta P_M]^2} \quad (37)$$

$$v_c=D_M+\sum n\Delta v_M \quad (38)$$

$$\omega=\frac{(T_b-43)(T_c-43)}{(T_c-T_b)(0.7T_c-43)}\log\left[\frac{P_c}{P_b}\right]-\frac{(T_b-43)}{(T_c-T_b)}\log\left[\frac{P_c}{P_b}\right]+\log\left[\frac{P_c}{P_b}\right]-1 \quad (39)$$

wherein $\Delta T_{bM}$, $\Delta T_M$, $\Delta v_M$ and $\Delta P_M$ are the model parameters that can be found in the literature [32]. Moreover, $A_M$=0.5703, $B_M$=1.0121, $C_M$=0.2573, $D_M$=6.75. All the estimated parameters for the studied ILs, reported in Table 1.

More details about the obtained results and their verification may be found in the previous work [2].

### 2. The PC-SAFT EoS Pure Parameters

Five optimizable parameters, including (m, $\sigma$, $\varepsilon$, $\varepsilon^{A_iB_j}$, and $\kappa^{A_iB_j}$), should be fitted for every associating component while they reduce to three (m, $\sigma$, $\varepsilon$) for a non-associating one. To find these variables, usually, the model fits the experimental data of liquid densities and vapor pressures. As no experimental data exist for the investigated ILs, only the liquid density data was used through the following cost function:

$$OF=\frac{100}{N_p}\sum_i^{N_p}\frac{\left|\rho_i^{exp}-\rho_i^{calc}\right|}{\rho_i^{exp}} \quad (40)$$

Pure $CO_2$ and $H_2S$ parameters were taken from the literature [33,

**Table 1. Estimated physical properties for the pure components using mLJR method**

| Component | $T_c$ (K) | $P_c$ (bar) | $v_c$ (cm$^3$/mol) | $\omega$ | $M_w$ |
|---|---|---|---|---|---|
| [DMEAH][Ac] | 692.80 | 35.06 | 458.41 | 0.94 | 135.1600 |
| [DMEAH][For] | 565.60 | 40.86 | 404.61 | 0.84 | 121.1327 |
| [MDEAH][Ac] | 783.96 | 37.37 | 479.11 | 1.34 | 151.1640 |
| [MDEAH][For] | 660.94 | 43.80 | 425.31 | 1.26 | 137.1317 |
| $CO_2$ | 304.13 | 73.85 | --- | 0.22 | 44.0095 |
| $H_2S$ | 373.10 | 90.00 | --- | 0.10 | 34.0820 |

**Table 2. Adjusted PC-SAFT parameters of pure components for ILs and gases**

| Component | m | $\sigma$ (A) | $\varepsilon$/k (K) | $\kappa^{A_iB_j}$ | $\varepsilon^{A_iB_j}$/k (K) | $N_p$ | Ref. | AAD%* (For IL density) |
|---|---|---|---|---|---|---|---|---|
| [DMEAH][Ac] | 2.6421 | 4.1006 | 305.5337 | 0.0025 | 3,392.7948 | 12 | This work | 0.0101 |
| [DMEAH][For] | 2.3637 | 4.1031 | 362.0474 | 0.0020 | 4,120.4660 | 12 | This work | 0.0132 |
| [MDEAH][Ac] | 2.8093 | 4.1455 | 330.7674 | 0.0024 | 3,599.1562 | 12 | This work | 0.0116 |
| [MDEAH][For] | 2.1959 | 4.4205 | 540.6711 | 0.0013 | 3,659.1829 | 12 | This work | 0.0156 |
| $CO_2$ | 2.729 | 2.7852 | 169.21 | --- | --- | --- | [20] | --- |
| $H_2S$ | 1.616 | 3.084 | 231.61 | 0.00125 | 417.69 | --- | [21] | --- |

*$AAD\% = \frac{100}{N_p}\sum_i^{N_p}\frac{\left|\rho_i^{exp}-\rho_i^{calc}\right|}{\rho_i^{exp}}$

34].

Where $N_p$ denotes the total number of data points. Experimental densities for all of the ionic liquids were obtained from the literature [35]. The adjusted parameters along with AAD% values of the used ILs have been reported in Table 2. According to the calculated results, PC-SAFT presents excellent accuracy in estimation of the density so that the densities of all the ILs have been computed with AADs% below 0.02. The experimental and calculated liquid densities of the ILs in various temperatures are plotted in Fig. 2. Detailed values are presented in Table S1 (Supporting Information).

## 3. Binary Systems

The first step for modeling the absorption of acidic gases into ILs is to find liquid phase concentrations. To do this, two different approaches were followed. The first one is to use experimental liquid concentration data, while the other way tries to compute them through CFR. As one can expect, the latest method needs an extra step for solving CFR. Actually, the first step is to compute the liquid mole fractions using CFR and the latest belongs to VLE calculations by PC-SAFT to obtain the pressure of the bubble point together with the vapor phase composition. $K_2$ and H parameters were taken from the literature [2] and correlated as a uniform function

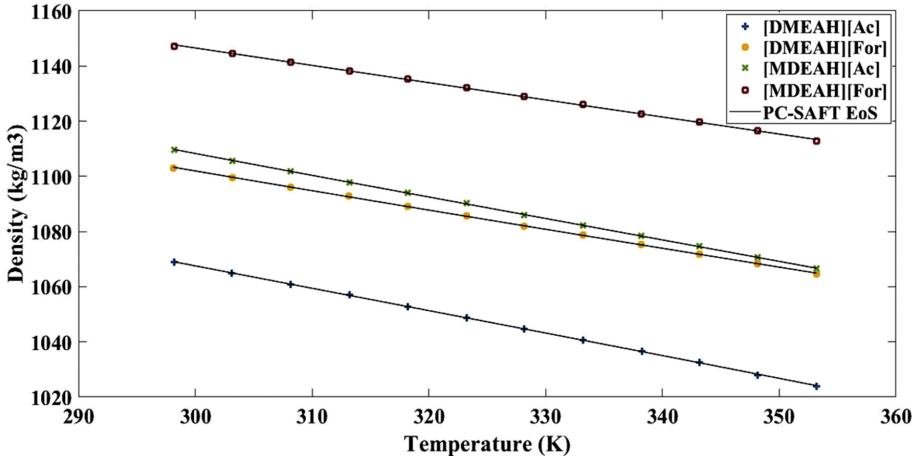


**Fig. 2. Experimental and calculated liquid densities of the ionic liquids in various temperatures using PC-SAFT EoS.**

**Table 3. Optimized parameters of the CFR for the IL+$CO_2$ and IL+$H_2S$ binary systems**

| Binary | Parameter | Coefficients of Eq. (41)* | | | | AAD%** (For IL molality) |
|---|---|---|---|---|---|---|
| | | A | B | C | D | |
| [DMEAH][Ac]+$CO_2$ | $K\times10^{-3}$ | −0.0420 | 0.0001 | 4.0616 | −0.0001 | 4.40 |
| | H (bar) | −15.6125 | 0.0555 | 395.2506 | −0.0939 | |
| [DMEAH][Ac]+$H_2S$ | $K\times10^{-3}$ | −0.0539 | 0.0001 | 9.3835 | 0.0001 | 4.91 |
| | H (bar) | −16.9996 | 0.0602 | −557.9932 | 0.1162 | |
| [DMEAH][For]+$CO_2$ | $K\times10^{-3}$ | 0.0236 | −0.0002 | −18.4357 | 0.0178 | 4.42 |
| | H (bar) | −64.1185 | 0.3346 | 16399.7644 | −15.4436 | |
| [DMEAH][For]+$H_2S$ | $K\times10^{-3}$ | 0.0328 | −0.0002 | −17.3834 | 0.0174 | 4.30 |
| | H (bar) | −65.6448 | 0.4357 | 9512.2367 | −16.8283 | |
| [MDEAH][Ac]+$CO_2$ | $K\times10^{-3}$ | −0.1223 | −0.0020 | 146.0216 | 0.2106 | 4.63 |
| | H (bar) | 21.1300 | 0.0277 | −2786.6019 | −3.2188 | |
| [MDEAH][Ac]+$H_2S$ | $K\times10^{-3}$ | 0.0123 | $3\times10^{-6}$ | 0.9279 | −0.0035 | 4.45 |
| | H (bar) | 23.5092 | 0.0156 | −6032.7010 | −1.3586 | |
| [MDEAH][For]+$CO_2$ | $K\times10^{-3}$ | −0.0131 | −0.00003 | −0.00002 | −0.00001 | 13.54 |
| | H (bar) | −2.3084 | 0.0172 | −2.0818 | −0.0454 | |
| [MDEAH][For]+$H_2S$ | $K\times10^{-3}$ | −0.0377 | 0.00007 | 8.7547 | −0.0003 | 4.48 |
| | H (bar) | −2.0719 | 0.0206 | −171.9824 | −0.2740 | |

*All the coefficients were taken from [2].

$$**\ \mathrm{AAD\%} = \frac{100}{N_p}\frac{\left|m_{A_0}^{Exp.} - m_{A_0}^{Calc.}\right|}{m_{A_0}^{Exp.}}$$

**Table 4. Binary interaction parameters for solubility of the acid gases in the ILs using PC-SAFT EoS with and without applying the CFR**

| Binary | PC-SAFT (Without CFR) | | | | | PC-SAFT (With CFR) | | | | |
|---|---|---|---|---|---|---|---|---|---|---|
| | a | b | c | $\kappa^{Cross.}$* | AAD%** (For total pressure) | a | b | c | $\kappa^{Cross.}$* | AAD%** (For total pressure) |
| [DMEAH][Ac]+$CO_2$ | −2.2301 | 0.0043 | 320.4504 | −0.4128 | **5.11** | −2.5294 | 0.0053 | 312.2902 | 0.0785 | **0.15** |
| [DMEAH][Ac]+$H_2S$ | −3.8589 | 0.0067 | 520.5075 | --- | **8.71** | −3.9991 | 0.0090 | 365.7770 | --- | **1.02** |
| [DMEAH][For]+$CO_2$ | 0.0002 | 0.0005 | −0.0001 | 0.0981 | **4.14** | −17.4593 | 0.0318 | 2,429.2690 | 0.0021 | **0.36** |
| [DMEAH][For]+$H_2S$ | −3.8841 | 0.0064 | 569.4749 | --- | **10.37** | −39.1202 | 0.0744 | 5,045.0001 | --- | **2.79** |
| [MDEAH][Ac]+$CO_2$ | −2.1440 | 0.0039 | 322.3603 | 0.0497 | **4.79** | −2.4891 | 0.0051 | 313.4102 | 0.0431 | **0.15** |
| [MDEAH][Ac]+$H_2S$ | −3.9094 | 0.0065 | 568.2691 | --- | **7.66** | −4.0359 | 0.0089 | 403.7807 | --- | **0.84** |
| [MDEAH][For]+$CO_2$ | −0.5953 | 0.0011 | 128.8935 | −1.2429 | **6.24** | −0.6656 | 0.0012 | 135.2690 | 0.0152 | **0.03** |
| [MDEAH][For]+$H_2S$ | −1.2702 | 0.0021 | 195.6693 | --- | **7.06** | −1.1864 | 0.0023 | 186.5445 | --- | **0.76** |

*This cross-association parameter adjusted for $CO_2$ containing systems only.

**$\mathrm{AAD\%} = \frac{100}{N_p}\sum_i^N \left|\frac{P^{cal} - P^{exp}}{P^{exp}}\right|$

***All the presented results have been obtained in the present work.

in terms of operating temperature as below:

$$\ln(H(\mathrm{bar})/K_2) = A + BT + \frac{C}{T} + D\ln(T) \tag{41}$$

The coefficients of Eq. (41) are reported in Table 3.

To determine the binary interaction parameters, a nonlinear simple form relation was considered as a function of temperature:

$$K_{i,j} = a + bT + \frac{c}{T} \tag{42}$$

The coefficients of Eq. (42) were obtained through minimizing the following cost function and all of them are presented in Table 4.

$$OF = \frac{100}{N_p}\sum_i^N \left|\frac{P^{cal} - P^{exp}}{P^{exp}}\right| \tag{43}$$

$P^{cal}$ and $P^{exp}$ represent computed and experimental pressures, respectively.

All the calculated pressure values have been presented in detail in the Supporting Information file.

Based on the presented results in the table, CFR could impressively promote correlation accuracy. Indeed, the combination of the CFR and the PC-SAFT EoS leads to overall AAD% equal to 0.89 for all the surveyed systems, while without CFR, this value increases to 6.88. Actually, CFR can cause an almost 90% improvement in the overall AAD%.

Elliott's combining rule (ECR) (Eq. (44)) was used to model $H_2S$ solubility, while the modified CR-1 combining rule (Eq. (45)) was applied for $CO_2$ as a non-self-associating component [36].

$$\varepsilon^{A_iB_j} = \frac{\varepsilon^{A_iB_i} + \varepsilon^{A_jB_j}}{2};\ \kappa^{A_iB_j} = \sqrt{\kappa^{A_iB_i}\kappa^{A_jB_j}}\left(\frac{\sqrt{\sigma_i\sigma_j}}{\sigma_{ij}}\right)^3 \tag{44}$$

$$\varepsilon^{A_iB_j} = \frac{\varepsilon_{IL}}{2};\ \kappa^{A_iB_j} = \mathrm{fitted} \tag{45}$$

The fitted values are reported in Table 4.

**Table 5. Comparison between the results of PC-SAFT, CPA and mSRK EoSs for correlating acid gas solubility in the ILs**

| Binaries | Overall AADs% for total pressure* | | |
|---|---|---|---|
| | PC-SAFT+CFR | CPA+CFR | mSRK |
| [DMEAH][Ac]+$CO_2$ | 0.15 | 0.21 | 2.52 |
| [DMEAH][Ac]+$H_2S$ | 1.02 | 1.50 | 5.29 |
| [DMEAH][For]+$CO_2$ | 0.36 | 0.40 | 2.17 |
| [DMEAH][For]+$H_2S$ | 2.79 | 2.98 | 7.33 |
| [MDEAH][Ac]+$CO_2$ | 0.15 | 0.21 | 4.57 |
| [MDEAH][Ac]+$H_2S$ | 0.84 | 0.77 | 7.66 |
| [MDEAH][For]+$CO_2$ | 0.03 | 0.11 | 4.14 |
| [MDEAH][For]+$H_2S$ | 0.76 | 0.73 | 4.17 |
| **Overall** | **0.80** | **0.92** | **4.77** |
| **Reference** | **This work** | **[2]** | **[2]** |

*$\mathrm{AAD\%} = \frac{100}{N_p}\sum_i^N \left|\frac{P^{cal} - P^{exp}}{P^{exp}}\right|$

In the previous work [2], the CPA, and the mSRK EoSs by Yokozeki and Schiflett [27], were used to model the present systems. For the sake of difference in the approaches used in the two works, a precise comparison cannot be accomplished. But Table 5 presents a rough comparison between the studied models.

Based on the results, the PC-SAFT demonstrates minimum mean overall AAD%=0.8 for both $CO_2$ and $H_2S$ included systems. On the other hand, CPA shows a bit better accuracy in a few cases. As a result, despite lower AAD% of the PC-SAFT, no meaningful difference can be seen between this model and the CPA, in the case of acid gas solubility estimation. This could be because of two reasons. At first, both PC-SAFT and CPA are of the association models family and can take into account the possible hydrogen bonding effects. Second, might be for the sake of using CFR. Indeed, both CFR and the association term can have a high impact on the model's

accuracy.

Another advantage of the PC-SAFT in comparison with the CPA and mSRK is that PC-SAFT does not need critical properties of the components. This will be more important when experimental data of such properties are not available. However, according to the accomplished sensitivity analysis in the previous work [2], CPA and

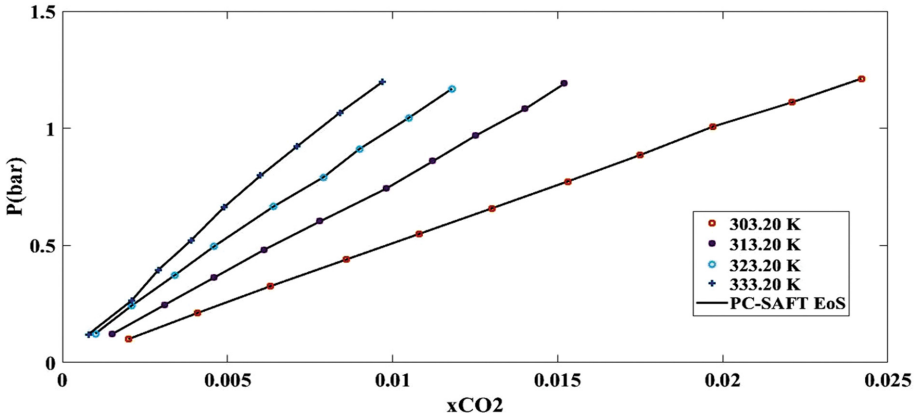


**Fig. 3. The experimental and calculated total pressures versus $CO_2$ liquid mole fractions in ionic liquid [DMEAH][Ac] at different temperatures using PC-SAFT EoS.**

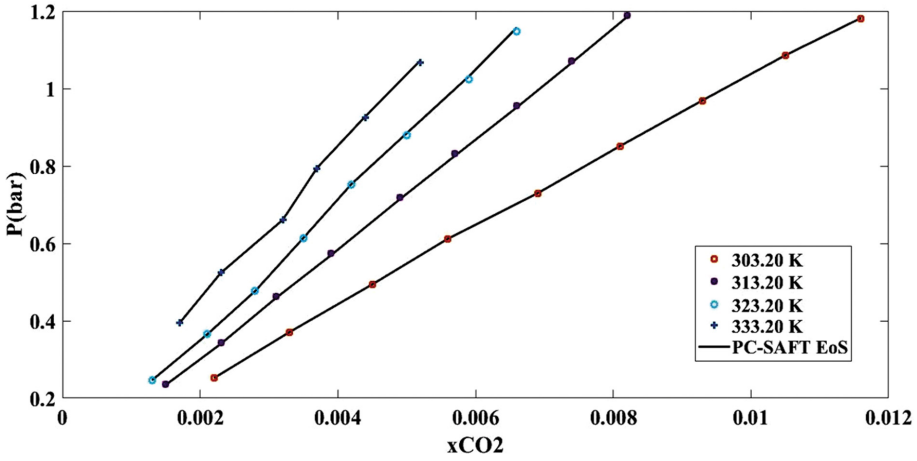


**Fig. 4. The experimental and calculated pressure versus $CO_2$ liquid mole fractions in ionic liquid [DMEAH][For] at different temperatures using PC-SAFT EoS.**

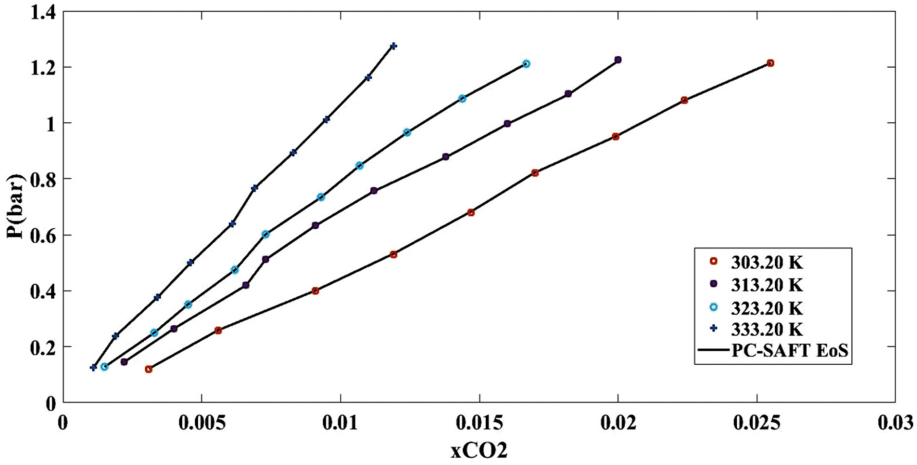


**Fig. 5. The experimental and calculated pressure versus $CO_2$ liquid mole fractions in ionic liquid [MDEAH][Ac] at different temperatures using PC-SAFT EoS.**

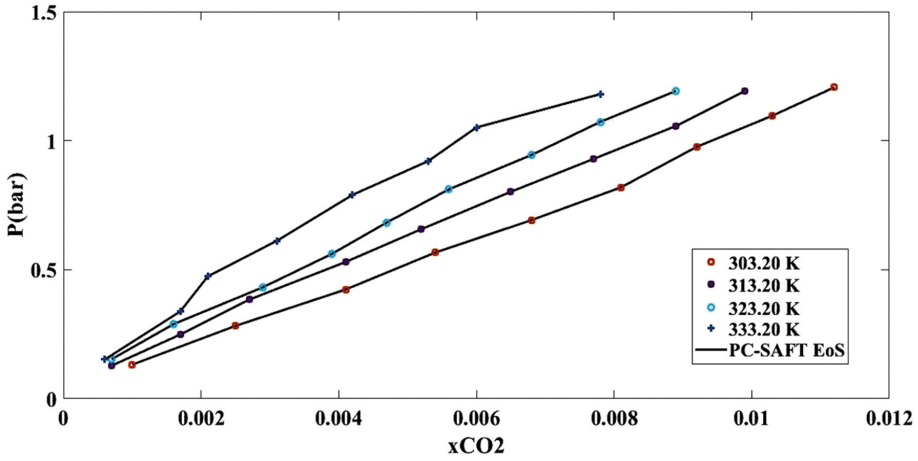


**Fig. 6. The experimental and calculated pressure versus $CO_2$ liquid mole fractions in ionic liquid [MDEAH][For] at different temperatures using PC-SAFT EoS.**

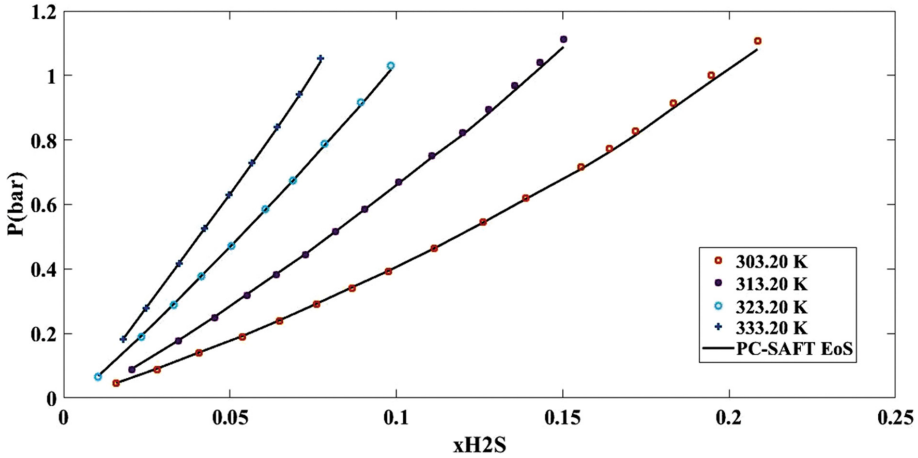


**Fig. 7. The experimental and calculated pressure versus $H_2S$ liquid mole fractions in ionic liquid [DMEAH][Ac] at different temperatures using PC-SAFT EoS.**

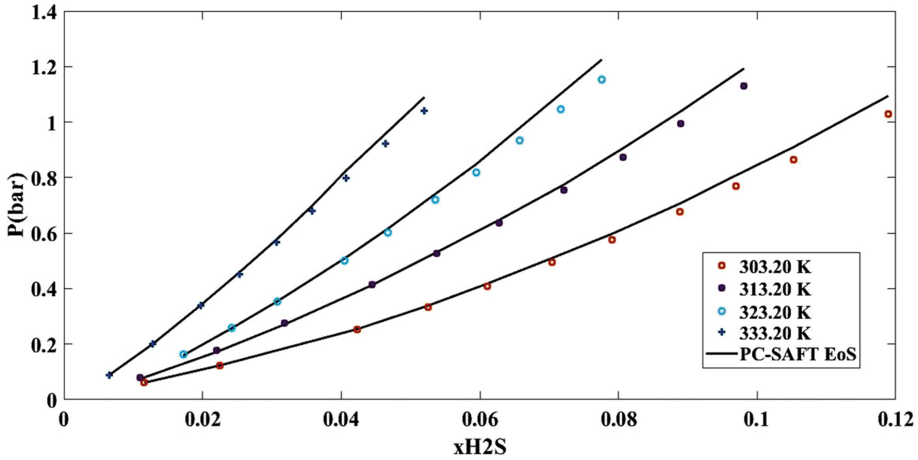


**Fig. 8. The experimental and calculated pressure versus $H_2S$ liquid mole fractions in ionic liquid [DMEAH][For] at different temperatures using PC-SAFT EoS.**

mSRK show very low sensitivity towards the accuracy of the estimated values.

Figs. 3 to 6 demonstrate total pressures versus the experimental and computed (by PC-SAFT) $CO_2$ mole fractions in [DMEAH]

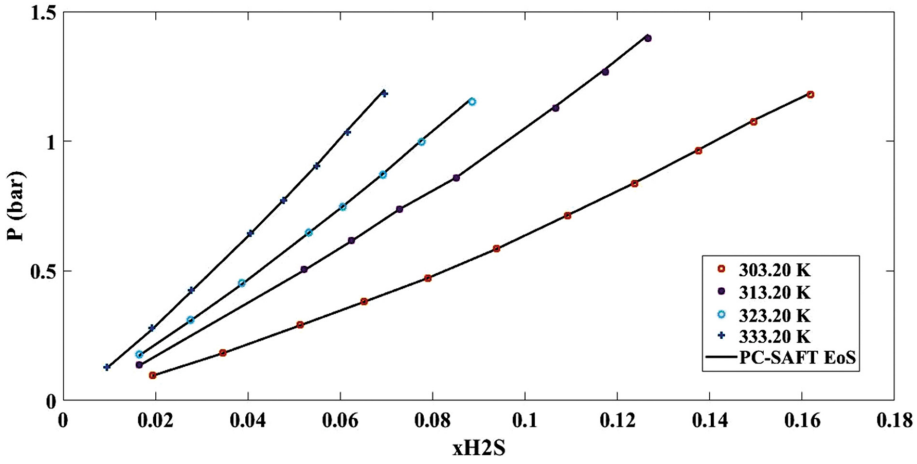


**Fig. 9. The experimental and calculated pressure versus $H_2S$ liquid mole fractions in ionic liquid [MDEAH][Ac] at different temperatures using PC-SAFT EoS.**

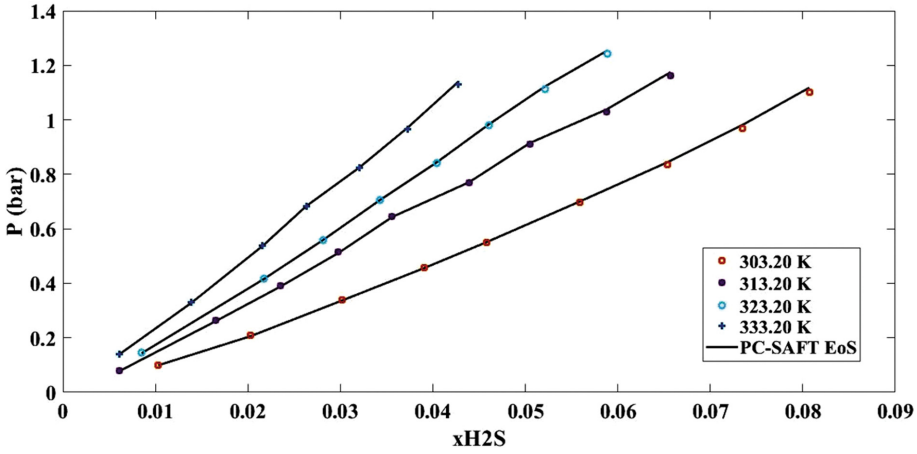


**Fig. 10. The experimental and calculated pressure versus $H_2S$ liquid mole fractions in ionic liquid [MDEAH][For] at different temperatures using PC-SAFT EoS.**

**Table 6. The adjusted parameters of the FVT model in combination with PC-SAFT/CPA/mSRK EoSs for the studied ILs**

| Model | Ionic liquid | The FVT parameters | | | Reference |
|---|---|---|---|---|---|
| | | L (m) | $E_0$ (kJ·mol$^{-1}$) | B | |
| PC-SAFT+FVT | [DMEAH][Ac] | 0.5178 | 20.7985 | 0.6114 | This work |
| | [DMEAH][For] | 3.4807 | 15.7228 | 0.7154 | |
| | [MDEAH][Ac] | 0.1584 | 19.2067 | 0.7853 | |
| | [MDEAH][For] | 0.4556 | 18.7498 | 0.8174 | |
| CPA+FVT | [DMEAH][Ac] | 0.5178 | 20.8116 | 0.6114 | This work |
| | [DMEAH][For] | 3.2875 | 21.3572 | 0.5288 | |
| | [MDEAH][Ac] | 0.1570 | 18.9575 | 0.7954 | |
| | [MDEAH][For] | 0.4517 | 18.7109 | 0.8196 | |
| mSRK+FVT | [DMEAH][Ac] | 0.0008 | 9.7169 | 3.5548 | This work |
| | [DMEAH][For] | 0.0011 | 24.8329 | 0.7216 | |
| | [MDEAH][Ac] | 0.0001 | 29.5698 | 0.8335 | |
| | [MDEAH][For] | 0.0002 | 30.0120 | 0.7836 | |

[Ac], [DMEAH][For], [MDEAH][Ac], and [MDEAH][For] ILs at various temperatures.

Figs. 7 to 10 exhibit solubility of $H_2S$ in the investigated ILs, respectively. According to these figures, a very good performance of the

PC-SAFT is seen.

## 4. Viscosity of the Ionic Liquids

FVT was mixed with the PC-SAFT/CPA/mSRK EoSs to estimate the dynamic viscosity of the investigated ILs. In this way, a new approach was followed. In the approach, the density of the ILs is calculated through the EoSs and then the obtained values are utilized to calculate $\Delta\eta$ in Eq. (30). Thus, the densities are obtained using the adjusted parameters in section 3.2. Then, these values are employed to estimate viscosities through optimizing three parameters related to the FVT. The obtained parameters of the FVT model have been reported in Table 6. A comparison between the results of the applied models is presented in Table 7. As anybody can observe, overall AADs% equal to 2.55, 2.52, and 2.59 were obtained using PC-SAFT, CPA, and mSRK, respectively.

Based on the achieved results, no significant discrepancy is observed between the used EoSs. It could be justified by the fact that the FVT model has enough correlative parameters to calculate viscosities using even a rough estimation of density values. As all the used EoSs can correlate the density of the ILs with enough accuracy, the final obtained viscosity results are very close to each other. This low sensitivity of the FVT to the used EoS could be considered as a distinguished positive characteristic of the model.

The experimental versus calculated viscosities of the ionic liquids using PCSAFT+FVT at different temperatures have been shown in Fig. 11.

**Table 7. Comparison between the accuracy of the estimated viscosities of the pure ILs using combination of PC-SAFT/CPA/mSRK EoSs and the FVT model**

| IL | Overall AADs% for the ILs viscosities* | | |
|---|---|---|---|
| | PC-SAFT+FVT | CPA+FVT | mSRK+FVT |
| [DMEAH][Ac] | 1.73 | 1.73 | 1.75 |
| [DMEAH][For] | 2.00 | 1.97 | 2.07 |
| [MDEAH][Ac] | 3.49 | 3.44 | 3.50 |
| [MDEAH][For] | 3.00 | 2.94 | 3.04 |
| **Overall** | **2.55** | **2.52** | **2.59** |
| **Reference** | **This work** | **This work** | **This work** |

$$*\mathrm{AAD}\% = \frac{100}{N_p}\sum_{i}^{N}\left|\frac{\eta^{cal}-\eta^{exp}}{\eta^{exp}}\right|$$

## 5. Model Predictability

To check the predictability of the models used for equilibrium data and viscosity calculations, a scenario was followed. In this way, for equilibrium calculation, between investigated temperatures including 303, 313, 323 and 333 K, two of them (303 and 333 K) were selected to obtain the model parameters (Correlation part). Data

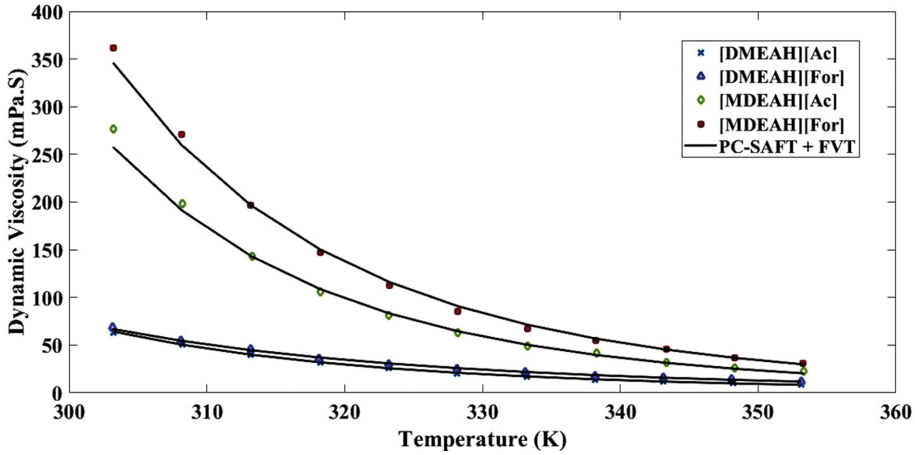


**Fig. 11. The experimental and calculated dynamic viscosities of the ionic liquids using PCSAFT+FVT at different temperatures.**

**Table 8. AADs% for prediction of equilibrium data for different binaries**

| Binaries | AAD% | | Binary interaction parameters | | | |
|---|---|---|---|---|---|---|
| | Correlation (303 & 333 K) | Prediction (313 & 323 K) | $a\times10^{-2}$ | $b\times10^{-2}$ | $c\times10^{-2}$ | $\kappa^{Cross.}$ |
| [DMEAH][Ac]+$CO_2$ | 0.15 | 0.19 | −0.025480 | 0.000053 | 3.153815 | 0.000736 |
| [DMEAH][Ac]+$H_2S$ | 0.98 | 1.05 | −0.040024 | 0.000090 | 3.663009 | --- |
| [DMEAH][For]+$CO_2$ | 0.81 | 17.86 | −0.064655 | 0.000145 | 6.849608 | 0.000861 |
| [DMEAH][For]+$H_2S$ | 1.84 | 34.33 | −0.137139 | 0.000345 | 10.118581 | --- |
| [MDEAH][Ac]+$CO_2$ | 0.11 | 0.13 | −0.023391 | 0.000049 | 2.891995 | 0.000505 |
| [MDEAH][Ac]+$H_2S$ | 0.82 | 0.87 | −0.040368 | 0.000089 | 4.039189 | --- |
| [MDEAH][For]+$CO_2$ | 0.03 | 0.029 | −0.006805 | 0.000013 | 1.37606 | 0.000156 |
| [MDEAH][For]+$H_2S$ | 0.79 | 0.73 | −0.012239 | 0.000023 | 1.924963 | --- |

**Table 9. AADs% for prediction of dynamic viscosities for different ILs**

| Binaries | AAD% | | FVT Parameters | | |
|---|---|---|---|---|---|
| | Correlation (6 data points) | Prediction (5 data points) | L (m) | $E_0$ (kJ·mol$^{-1}$) | B |
| [DMEAH][Ac] | 1.07 | 2.69 | 0.5910 | 20,820.7276 | 0.6020 |
| [DMEAH][For] | 0.86 | 3.80 | 3.2054 | 15,801.1873 | 0.7203 |
| [MDEAH][Ac] | 3.42 | 3.57 | 0.1617 | 21,464.1584 | 0.7061 |
| [MDEAH][For] | 2.65 | 3.74 | 0.4838 | 18,829.0486 | 0.8099 |

of the two other temperatures (313 and 323 K) were predicted using the obtained parameters in the correlation part. Table 8 presents obtained results for the equilibria calculations.

As one can see from the results, the used model presents good ability in both correlation and prediction approaches.

Following the latest approach, for prediction of dynamic viscosities, six experimental data were utilized to obtain model parameters (Correlation part) and the other five data were employed to check the model's predictability. In this way, data in 303.19, 313.19, 323.27, 333.26, 343.35 and 353.25 K were used for correlation scenario and those in 308.15, 318.23, 328.22, 338.21 and 348.30 K for the prediction part.

Table 9 presents obtained parameters and the results in both scenarios.

According to the obtained AADs%, it can be concluded that the PC-SAFT+FVT model has high ability in both correlation and prediction of viscosity values.

## CONCLUSIONS

A combination of the PC-SAFT EoS and CFR was employed to compute the acidic gas solubility in ionic liquids [DMEAH][Ac], [DMEAH][For], [MDEAH][Ac] and [MDEAH][For] through a VLE calculation approach. In this way, CFR calculates the liquid phase mole fractions and then PC-SAFT is implemented for the VLE calculation part.

Experimental density data of the ILs were utilized to find the PC-SAFT pure parameters. Accordingly, all the parameters were adjusted with excellent AADs% about 0.01 for all the ILs.

In addition, for the investigated binaries, including [DMEAH][Ac]+$CO_2$, [DMEAH][For]+$CO_2$, [MDEAH][Ac]+$CO_2$, [MDEAH][For]+$CO_2$, [DMEAH][Ac]+$H_2S$, [DMEAH][For]+$H_2S$, [MDEAH][Ac]+$H_2S$, and [MDEAH][For]+$H_2S$, the AADs% equal to 0.15, 0.36, 0.15, 0.03, 1.02, 2.79, 0.84 and 0.76 were found, respectively. Moreover, overall AADs% equal to 1.38 for $H_2S$ and 0.17 for $CO_2$ solubility were calculated. To show the CFR impact, results were obtained with and without using CFR. As the outputs present, meaningful improvement (from AAD%=6.88 to AAD%=0.8) is observed in the case of CFR use.

The PC-SAFT results were also compared with those of CPA and mSRK EoSs. Based on the results, the PC-SAFT and the CPA show close results so that using these models, 0.8 and 0.92 were obtained as total AADs%, respectively. This nearness can be because of the presence of the association term and the CFR.

In the next part of the work, the dynamic density of the studied ILs was estimated by merging the PC-SAFT, CPA and mSRK EoSs and the FVT model. In the followed approach, the density of the IL is calculated using the EoSs and then these values are utilized to compute viscosity. According to the results, all the implemented EoSs show very close AADs% equal to almost 2.5. This is because FVT has enough optimizable parameters by itself. Actually, it could be concluded that the FVT can present suitable accuracy with low sensitivity toward paired EoS.

## LIST OF SYMBOLS

$\tilde{a}$ : reduced Helmholtz energy
B : dimensionless constant of FVT model
d : temperature-dependent diameter [Å]
$E_0$ : free space formation parameter
g : radial distribution function
H : Henry's law constant
k : Boltzmann's constant (1.38066×10-23 J K$^{-1}$)
$K_i$ : equilibrium constant of reaction *i*
L : diffuse barrier energy
$\widehat{m}_i$ : molality of component I [mol/kg]
m : number of segments
$M_w$ : molecular weight
$N_P$ : number of data points
Ni : number of molecules of component *i*
$N_A$ : Avogadro's number [6.02205×10$^{23}$/mol]
P : total pressure
$P_b$ : boiling pressure
$P_C$ : critical pressure
R : universal gas constant [8.31415 J/mol·K]
$\beta$ : mSRK parameter
T : absolute temperature [K]
$T_b$ : normal boiling temperature [K]
$T_C$ : critical temperature [K]
Tr : reduced temperature [$T/T_c$]
v : molar volume
$v_C$ : critical volume
V : volume [m$^3$]
w : acentric factor
$X_{Ai}$ : fraction of A-type unbounded sites on molecule *i*
Z : compressibility factor

**Greek Letters**

$\Delta^{A_iB_j}$ : association strength
$\varepsilon_i$ : segment energy

$\varepsilon^{AB}$ : association energy
$\eta$ : dynamic viscosity [mPa·S]
$\kappa^{A_iB_j}$ : association volume
$\rho$ : density
$\sigma$ : temperature-independent diameter [Å]
$\xi$ : hard chain term parameter

**Superscript**

Assoc. : association
Cal. : calculated
disp. : dispersion
Exp. : experimental
hs. : hard sphere
hc : hard chain
res. : residual

## SUPPORTING INFORMATION

Additional information as noted in the text. This information is available via the Internet at http://www.springer.com/chemistry/journal/11814.

## REFERENCES


1. A. Afsharpour, *Chin. J. Chem. Eng.*, In press (2021).
2. A. Afsharpour, *J. Mol. Liq.*, **324**, 114684 (2021).
3. R. Macías-Salinas, J. A. Chávez-Velasco, M. A. Aquino-Olivos, J. L. Mendoza de la Cruz and J. C. Sánchez-Ochoa, *Ind. Eng. Chem. Res.*, **52**, 7593 (2013).
4. E. Voutsas, C. Perakis, G. Pappa and D. Tassios, *Fluid Phase Equilib.*, **261**, 343 (2007).
5. H. Al-fnaish and L. Lue, *Fluid Phase Equilib.*, **450**, 30 (2017).
6. X. Ji, C. Held and G. Sadowski, *Fluid Phase Equilib.*, **335**, 64 (2012).
7. X. Ji, C. Held and G. Sadowski, *Fluid Phase Equilib.*, **363**, 59 (2014).
8. N. Mac Dowell, F. E. Pereira, F. Llovell, F. J. Blas, C. S. Adjiman, G. Jackson and A. Galindo, *J. Phys. Chem. B*, **115**, 8155 (2011).
9. L.-T. Zhu, J.-X. Tang and Z.-H. Luo, *AIChE J.*, **66**, e16973 (2020).
10. W. Xiong, M. Shi, L. Peng, X. Zhang, X. Hu and Y. Wu, *Sep. Purif. Technol.*, **263**, 118417 (2021).
11. X. Zhang, W. Xiong, M. Shi, Y. Wu and X. Hu, *Chem. Eng. J.*, **408**, 127866 (2021).
12. F. Llovell, R. M. Marcos and L. F. Vega, *J. Phys. Chem. B*, **117**, 8159 (2013).
13. Y. Khoshnamvand and M. Assareh, *Int. J. Thermophys.*, **39**, 54 (2018).
14. G. Shen, C. Held, J.-P. Mikkola, X. Lu and X. Ji, *Ind. Eng. Chem. Res.*, **53**, 20258 (2014).
15. K. Huang, D.-N. Cai, Y.-L. Chen, Y.-T. Wu, X.-B. Hu and Z.-B. Zhang, *AIChE J.*, **59**, 2227 (2013).
16. J. Gross and G. Sadowski, *Ind. Eng. Chem. Res.*, **40**, 1244 (2001).
17. W. G. Chapman, G. Jackson and K. E. Gubbins, *Mol. Phys.*, **65**, 1057 (1988).
18. W. G. Chapman, K. E. Gubbins, G. Jackson and M. Radosz, *Ind. Eng. Chem. Res.*, **29**, 1709 (1990).
19. Y. C. Chiew, *Mol. Phys.*, **73**, 359 (1991).
20. J. Gross and G. Sadowski, *Fluid Phase Equilib.*, **168**, 183 (2000).
21. I. Senol, *Int. J. Mater. Metall. Eng.*, **5**, 940 (2011).
22. M. S. Wertheim, *J. Statistical Phys.*, **42**, 459 (1986).
23. M. S. Wertheim, *J. Statistical Phys.*, **35**, 35 (1984).
24. M. S. Wertheim, *J. Statistical Phys.*, **35**, 19 (1984).
25. M. S. Wertheim, *J. Statistical Phys.*, **42**, 477 (1986).
26. O. Redlich and J. N. S. Kwong, *Chem. Rev.*, **44**, 233 (1949).
27. M. Shiflett and A. Yokozeki, *Fluid Phase Equilib.*, **294**, 105 (2010).
28. G. M. Kontogeorgis, E. C. Voutsas, I. V. Yakoumis and D. P. Tassios, *Ind. Eng. Chem. Res.*, **35**, 4310 (1996).
29. A. Afsharpour, *Pet. Sci. Technol.*, **37**, 1648 (2019).
30. A. Allal, M. Moha-ouchane and C. Boned, *Phys. Chem. Liq.*, **39**, 1 (2001).
31. M. H. Cohen and D. Turnbull, *J. Chem. Phys.*, **31**, 1164 (1959).
32. J. O. Valderrama and P. A. Robles, *Ind. Eng. Chem. Res.*, **46**, 1338 (2007).
33. D. N. J.-G. Germán A. Ávila-Méndez, F. García-Sánchez and B. E. García-Flores, *Open Thermodynam. J.*, **5**, 7 (2011).
34. A. Raeispour Shirazi and M. N. Lotfollahi, *Fluid Phase Equilib.*, **502**, 112289 (2019).
35. K. Huang, X.-M. Zhang, Y. Xu, Y.-T. Wu, X.-B. Hu and Y. Xu, *AIChE J.*, **60**, 4232 (2014).
36. G. M. Kontogeorgis and G. K. Folas, *Thermodynamic models for industrial applications: From classical and advanced mixing rules to association theories*, Wiley, United Kingdom (2009).

# Supporting Information

# Application of PC-SAFT EoS for calculating gas solubility and viscosity of ammonium-based ionic liquids

**Alireza Afsharpour† and Seyyed Hamid Esmaeli-Faraj**

Faculty of Chemical and Materials Engineering, Shahrood University of Technology, Shahrood, Iran
(*Received 17 August 2021 • Revised 5 January 2022 • Accepted 19 January 2022*)

**Table S1. Experimental and calculated densities of the ILs in various temperatures**

| Temperature (K) | Liquid density ($kg/m^3$) | | | | | | | | | | | |
|---|---|---|---|---|---|---|---|---|---|---|---|---|
| | [DMEAH][AC] | | | [DMEAH][For] | | | [MDEAH][Ac] | | | [MDEAH][For] | | |
| | Calc. | Exp. | AAD% | Calc. | Exp. | AAD% | Calc. | Exp. | AAD% | Calc. | Exp. | AAD% |
| 298.21 | 1,069.02 | 1,068.90 | 0.011 | 1,103.33 | 1,103.10 | 0.021 | 1,109.73 | 1,109.50 | 0.021 | 1,147.69 | 1,147.29 | 0.035 |
| 303.15 | 1,065.00 | 1,065.00 | 0.000 | 1,099.70 | 1,099.50 | 0.018 | 1,105.79 | 1,105.60 | 0.017 | 1,144.56 | 1,144.46 | 0.008 |
| 308.19 | 1,060.91 | 1,060.90 | 0.001 | 1,096.10 | 1,096.10 | 0.000 | 1,101.80 | 1,101.80 | 0.000 | 1,141.37 | 1,141.37 | 0.000 |
| 313.24 | 1,056.82 | 1,057.00 | 0.017 | 1,092.59 | 1,092.80 | 0.019 | 1,097.83 | 1,097.90 | 0.006 | 1,138.20 | 1,138.29 | 0.008 |
| 318.18 | 1,052.81 | 1,052.90 | 0.008 | 1,089.05 | 1,089.20 | 0.014 | 1,093.95 | 1,094.10 | 0.014 | 1,135.10 | 1,135.20 | 0.009 |
| 323.22 | 1,048.72 | 1,048.80 | 0.007 | 1,085.52 | 1,085.60 | 0.007 | 1,090.01 | 1,090.20 | 0.017 | 1,131.95 | 1,132.11 | 0.014 |
| 328.16 | 1,044.71 | 1,044.70 | 0.001 | 1,082.09 | 1,082.00 | 0.008 | 1,086.16 | 1,086.10 | 0.006 | 1,128.87 | 1,129.03 | 0.014 |
| 333.21 | 1,040.60 | 1,040.60 | 0.000 | 1,078.60 | 1,078.60 | 0.000 | 1,082.24 | 1,082.20 | 0.003 | 1,125.74 | 1,125.94 | 0.018 |
| 338.25 | 1,036.48 | 1,036.50 | 0.002 | 1,075.20 | 1,075.30 | 0.009 | 1,078.40 | 1,078.40 | 0.000 | 1,122.67 | 1,122.60 | 0.006 |
| 343.19 | 1,032.42 | 1,032.60 | 0.018 | 1,071.75 | 1,071.90 | 0.014 | 1,074.49 | 1,074.80 | 0.029 | 1,119.55 | 1,119.77 | 0.020 |
| 348.14 | 1,028.33 | 1,028.00 | 0.032 | 1,068.36 | 1,068.30 | 0.006 | 1,070.64 | 1,070.70 | 0.006 | 1,116.49 | 1,116.43 | 0.006 |
| 353.18 | 1,024.14 | 1,023.90 | 0.024 | 1,064.93 | 1,064.50 | 0.040 | 1,066.72 | 1,066.50 | 0.020 | 1,113.38 | 1,112.83 | 0.049 |

**Table S2. Experimental and calculated Pressures for [DMEAH][AC]+$CO_2$ system in various temperatures**

| [DMEAH][For]+$CO_2$ | | | | | | | | | | | | |
|---|---|---|---|---|---|---|---|---|---|---|---|---|
| T=303.2 K | | | T=313.2 K | | | T=323.2 K | | | T=333.2 K | | |
| $P^{Calc.}$ (Pa) | $P^{Exp.}$ (Pa) | AAD% | $P^{Calc.}$ (Pa) | $P^{Exp.}$ (Pa) | AAD% | $P^{Calc.}$ (Pa) | $P^{Exp.}$ (Pa) | AAD% | $P^{Calc.}$ (Pa) | $P^{Exp.}$ (Pa) | AAD% |
| 25,195.06 | 25,200 | 0.020 | 23,430.47 | 23,700 | 1.137 | 24,631.50 | 24,700 | 0.277 | 39,413.16 | 39,500 | 0.220 |
| 37,098.04 | 37,100 | 0.005 | 34,041.35 | 34,400 | 1.043 | 36,450.34 | 36,500 | 0.136 | 52,368.50 | 52,400 | 0.060 |
| 49,404.81 | 49,400 | 0.010 | 45,866.61 | 46,300 | 0.936 | 47,700.40 | 47,700 | 0.001 | 66,073.56 | 66,000 | 0.111 |
| 61,214.77 | 61,200 | 0.024 | 56,920.07 | 57,400 | 0.836 | 61,403.45 | 61,300 | 0.169 | 79,522.88 | 79,300 | 0.281 |
| 72,927.94 | 72,900 | 0.038 | 71,393.01 | 71,900 | 0.705 | 75,355.58 | 75,100 | 0.340 | 92,815.15 | 92,400 | 0.449 |
| 85,145.11 | 85,100 | 0.053 | 82,598.32 | 83,100 | 0.604 | 88,441.24 | 88,000 | 0.501 | 107,274.47 | 106,600 | 0.633 |
| 96,965.01 | 96,900 | 0.067 | 95,131.26 | 95,600 | 0.490 | 103,098.28 | 102,400 | 0.682 | --- | --- | --- |
| 108,587.68 | 108,500 | 0.081 | 106,686.77 | 107,100 | 0.386 | 115,761.87 | 114,800 | 0.838 | --- | --- | --- |
| 118,208.74 | 118,100 | 0.092 | 118,468.08 | 118,800 | 0.279 | --- | --- | --- | --- | --- | --- |
| 10,015.92 | 10,000 | 0.159 | --- | --- | --- | --- | --- | --- | --- | --- | --- |

**Table S3. Experimental and calculated pressures for [DMEAH][For]+$CO_2$ system in various temperatures**

| [DMEAH][AC]+$CO_2$ | | | | | | | | | | | |
|---|---|---|---|---|---|---|---|---|---|---|---|
| T=303.2 K | | | T=313.2 K | | | T=323.2 K | | | T=333.2 K | | |
| $P^{Calc.}$ (Pa) | $P^{Exp.}$ (Pa) | AAD% | $P^{Calc.}$ (Pa) | $P^{Exp.}$ (Pa) | AAD% | $P^{Calc.}$ (Pa) | $P^{Exp.}$ (Pa) | AAD% | $P^{Calc.}$ (Pa) | $P^{Exp.}$ (Pa) | AAD% |
| 10,015.92 | 10,000 | 0.159 | 12,105.03 | 12,100 | 0.042 | 12,368.68 | 12,300 | 0.558 | 12,191.75 | 12,000 | 1.598 |
| 21,208.14 | 21,200 | 0.038 | 24,653.65 | 24,700 | 0.188 | 24,320.75 | 24,300 | 0.085 | 26,510.29 | 26,400 | 0.418 |
| 32,602.94 | 32,600 | 0.009 | 36,310.93 | 36,400 | 0.245 | 37,284.16 | 37,300 | 0.042 | 39,454.47 | 39,400 | 0.138 |
| 44,000.00 | 44,000 | 0.000 | 48,072.52 | 48,200 | 0.264 | 49,664.01 | 49,700 | 0.072 | 52,215.91 | 52,200 | 0.030 |
| 54,898.87 | 54,900 | 0.002 | 60,237.58 | 60,400 | 0.269 | 66,659.60 | 66,700 | 0.061 | 66,392.13 | 66,400 | 0.012 |
| 65,798.98 | 65,800 | 0.002 | 74,203.20 | 74,400 | 0.265 | 79,073.19 | 79,100 | 0.034 | 79,787.99 | 79,800 | 0.015 |
| 77,300.00 | 77,300 | 0.000 | 85,779.15 | 86,000 | 0.257 | 91,200.00 | 91,200 | 0.000 | 92,199.96 | 92,200 | 0.000 |
| 88,601.46 | 88,600 | 0.002 | 96,759.91 | 97,000 | 0.248 | 104,544.80 | 104,500 | 0.043 | 106,632.87 | 106,600 | 0.031 |
| 100,703.03 | 100,700 | 0.003 | 108,143.47 | 108,400 | 0.237 | 116,900.42 | 116,800 | 0.086 | 119,880.97 | 119,800 | 0.068 |
| 111,104.00 | 111,100 | 0.004 | 119,030.95 | 119,300 | 0.226 | 12,368.68 | 12,300 | 0.558 | 12,191.75 | 12,000 | 1.598 |
| 121,204.28 | 121,200 | 0.004 | 12,105.03 | 12,100 | 0.042 | 24,320.75 | 24,300 | 0.085 | 26,510.29 | 26,400 | 0.418 |
| 10,015.92 | 10,000 | 0.159 | 24,653.65 | 24,700 | 0.188 | 37,284.16 | 37,300 | 0.042 | 39,454.47 | 39,400 | 0.138 |

**Table S4. Experimental and calculated pressures for [MDEAH][AC]+$CO_2$ system in various temperatures**

| [MDEAH][AC]+$CO_2$ | | | | | | | | | | | |
|---|---|---|---|---|---|---|---|---|---|---|---|
| T=303.2 K | | | T=313.2 K | | | T=323.2 K | | | T=333.2 K | | |
| $P^{Calc.}$ (Pa) | $P^{Exp.}$ (Pa) | AAD% | $P^{Calc.}$ (Pa) | $P^{Exp.}$ (Pa) | AAD% | $P^{Calc.}$ (Pa) | $P^{Exp.}$ (Pa) | AAD% | $P^{Calc.}$ (Pa) | $P^{Exp.}$ (Pa) | AAD% |
| 12,182.85 | 12,100 | 0.685 | 14,500.00 | 14,500 | 0.000 | 12,790.74 | 12,800 | 0.072 | 12,504.63 | 12,500 | 0.037 |
| 25,950.45 | 25,800 | 0.583 | 26,487.59 | 26,500 | 0.047 | 25,076.94 | 25,100 | 0.092 | 23,892.12 | 23,900 | 0.033 |
| 40,093.01 | 39,900 | 0.484 | 41,960.51 | 42,000 | 0.094 | 35,070.96 | 35,100 | 0.083 | 37,589.93 | 37,600 | 0.027 |
| 53,207.68 | 53,000 | 0.392 | 51,138.45 | 51,200 | 0.120 | 47,470.00 | 47,500 | 0.063 | 50,000.00 | 50,000 | 0.000 |
| 68,294.44 | 68,100 | 0.286 | 63,302.25 | 63,400 | 0.154 | 60,176.33 | 60,200 | 0.039 | 64,025.10 | 64,000 | 0.039 |
| 82,252.94 | 82,100 | 0.186 | 75,557.63 | 75,700 | 0.188 | 73,390.65 | 73,400 | 0.013 | 76,660.10 | 76,600 | 0.078 |
| 95,089.47 | 95,000 | 0.094 | 87,705.23 | 87,900 | 0.222 | 84,809.28 | 84,800 | 0.011 | 89,407.26 | 89,300 | 0.120 |
| 108,100.00 | 108,100 | 0.000 | 99,546.19 | 99,800 | 0.254 | 96,534.37 | 96,500 | 0.036 | 101,462.75 | 101,300 | 0.161 |
| 121,382.07 | 121,500 | 0.097 | 110,086.95 | 110,400 | 0.284 | 108,867.18 | 108,800 | 0.062 | 116,547.00 | 116,300 | 0.212 |
| --- | --- | --- | 122,111.58 | 122,500 | 0.317 | 121,206.50 | 121,100 | 0.088 | 127,820.67 | 127,500 | 0.252 |

**Table S5. Experimental and calculated pressures for [MDEAH][For]+$CO_2$ system in various temperatures**

| [MDEAH][For]+$CO_2$ | | | | | | | | | | | |
|---|---|---|---|---|---|---|---|---|---|---|---|
| T=303.2 K | | | T=313.2 K | | | T=323.2 K | | | T=333.2 K | | |
| $P^{Calc.}$ (Pa) | $P^{Exp.}$ (Pa) | AAD% | $P^{Calc.}$ (Pa) | $P^{Exp.}$ (Pa) | AAD% | $P^{Calc.}$ (Pa) | $P^{Exp.}$ (Pa) | AAD% | $P^{Calc.}$ (Pa) | $P^{Exp.}$ (Pa) | AAD% |
| 13,209.21 | 13,200 | 0.070 | 12,799.88 | 12,800 | 0.001 | 15,300.00 | 15,300 | 0.000 | 15,186.23 | 15,200 | 0.091 |
| 28,215.72 | 28,200 | 0.056 | 24,899.77 | 24,900 | 0.001 | 28,902.70 | 28,900 | 0.009 | 33,876.73 | 33,900 | 0.069 |
| 42,318.00 | 42,300 | 0.043 | 38,399.68 | 38,400 | 0.001 | 43,208.31 | 43,200 | 0.019 | 47,475.06 | 47,500 | 0.053 |
| 56,616.49 | 56,600 | 0.029 | 52,999.62 | 53,000 | 0.001 | 56,115.84 | 56,100 | 0.028 | 61,177.87 | 61,200 | 0.036 |
| 69,211.94 | 69,200 | 0.017 | 65,699.61 | 65,700 | 0.001 | 68,325.13 | 68,300 | 0.037 | 78,988.31 | 79,000 | 0.015 |
| 81,904.29 | 81,900 | 0.005 | 80,199.63 | 80,200 | 0.000 | 81,137.14 | 81,100 | 0.046 | 92,100.92 | 92,100 | 0.001 |
| 97,590.56 | 97,600 | 0.010 | 92,899.70 | 92,900 | 0.000 | 94,452.12 | 94,400 | 0.055 | 105,117.61 | 105,100 | 0.017 |
| 109,676.74 | 109,700 | 0.021 | 105,699.82 | 105,700 | 0.000 | 107,268.95 | 107,200 | 0.064 | 118,038.30 | 118,000 | 0.032 |
| 120,661.72 | 120,700 | 0.032 | 119,200.00 | 119,200 | 0.000 | 119,286.89 | 119,200 | 0.073 | 15,186.23 | 15,200 | 0.091 |
| 13,209.21 | 13,200 | 0.070 | 12,799.88 | 12,800 | 0.001 | 15,300.00 | 15,300 | 0.000 | 33,876.73 | 33,900 | 0.069 |
| 28,215.72 | 28,200 | 0.056 | 24,899.77 | 24,900 | 0.001 | 28,902.70 | 28,900 | 0.009 | 47,475.06 | 47,500 | 0.053 |
| 42,318.00 | 42,300 | 0.043 | 38,399.68 | 38,400 | 0.001 | 43,208.31 | 43,200 | 0.019 | --- | --- | --- |

**Table S6. Experimental and calculated pressures for [DMEAH][AC]+$H_2S$ system in various temperatures**

| [DMEAH][AC]+$H_2S$ | | | | | | | | | | | |
|---|---|---|---|---|---|---|---|---|---|---|---|
| T=303.2 K | | | T=313.2 K | | | T=323.2 K | | | T=333.2 K | | |
| $P^{Calc.}$ (Pa) | $P^{Exp.}$ (Pa) | AAD% | $P^{Calc.}$ (Pa) | $P^{Exp.}$ (Pa) | AAD% | $P^{Calc.}$ (Pa) | $P^{Exp.}$ (Pa) | AAD% | $P^{Calc.}$ (Pa) | $P^{Exp.}$ (Pa) | AAD% |
| 4,602.60 | 4,500 | 2.280 | 9,014.46 | 8,800 | 2.437 | 6,804.23 | 6,600 | 3.094 | 18,412.02 | 18,100 | 1.724 |
| 9,060.72 | 8,900 | 1.806 | 17,907.64 | 17,600 | 1.748 | 19,178.96 | 18,900 | 1.476 | 28,092.94 | 27,800 | 1.054 |
| 14,106.36 | 13,900 | 1.485 | 25,238.93 | 24,900 | 1.361 | 29,182.71 | 28,900 | 0.978 | 41,918.78 | 41,700 | 0.525 |
| 19,230.94 | 19,000 | 1.215 | 32,230.27 | 31,900 | 1.035 | 37,944.07 | 37,700 | 0.647 | 52,623.22 | 52,500 | 0.235 |
| 24,034.19 | 23,800 | 0.984 | 38,490.46 | 38,200 | 0.760 | 47,358.62 | 47,200 | 0.336 | 62,900.00 | 62,900 | 0.000 |
| 29,216.33 | 29,000 | 0.746 | 44,720.66 | 44,500 | 0.496 | 58,400.00 | 58,400 | 0.000 | 72,654.36 | 72,800 | 0.200 |
| 34,277.60 | 34,100 | 0.521 | 51,706.43 | 51,600 | 0.206 | 67,227.52 | 67,400 | 0.256 | 83,754.48 | 84,100 | 0.411 |
| 39,416.87 | 39,300 | 0.297 | 58,557.33 | 58,600 | 0.073 | 78,449.24 | 78,900 | 0.571 | 93,645.59 | 94,200 | 0.589 |
| 46,400.00 | 46,400 | 0.000 | 66,634.15 | 66,900 | 0.397 | 90,767.12 | 91,600 | 0.909 | 104,385.74 | 105,200 | 0.774 |
| 54,417.35 | 54,600 | 0.335 | 74,564.88 | 75,100 | 0.713 | 101,854.01 | 103,100 | 1.209 | --- | --- | --- |
| 61,706.65 | 62,100 | 0.633 | 81,488.95 | 82,300 | 0.985 | --- | --- | --- | --- | --- | --- |
| 70,977.706 | 71,700 | 1.007 | 88,376.54 | 89,500 | 1.255 | --- | --- | --- | --- | --- | --- |
| 76,259.971 | 77,200 | 1.218 | 95,322.97 | 96,800 | 1.526 | --- | --- | --- | --- | --- | --- |
| 81,521.345 | 82,700 | 1.425 | 102,232.7 | 104,100 | 1.794 | --- | --- | --- | --- | --- | --- |
| 89,896.917 | 91,500 | 1.752 | 108,824.5 | 111,100 | 2.048 | --- | --- | --- | --- | --- | --- |
| 98,126.859 | 100,200 | 2.069 | --- | --- | --- | --- | --- | --- | --- | --- | --- |
| 108,088.08 | 110,800 | 2.448 | --- | --- | --- | --- | --- | --- | --- | --- | --- |

**Table S7. Experimental and calculated pressures for [DMEAH][For]+$H_2S$ system in various temperatures**

| [DMEAH][For]+$H_2S$ | | | | | | | | | | | |
|---|---|---|---|---|---|---|---|---|---|---|---|
| T=303.2 K | | | T=313.2 K | | | T=323.2 K | | | T=333.2 K | | |
| $P^{Calc.}$ (Pa) | $P^{Exp.}$ (Pa) | AAD% | $P^{Calc.}$ (Pa) | $P^{Exp.}$ (Pa) | AAD% | $P^{Calc.}$ (Pa) | $P^{Exp.}$ (Pa) | AAD% | $P^{Calc.}$ (Pa) | $P^{Exp.}$ (Pa) | AAD% |
| 6,110.32 | 6,200 | 1.446 | 7,461.78 | 7,800 | 4.336 | 15,932.45 | 16,200 | 1.652 | 8,801.15 | 8,900 | 1.111 |
| 12,316.67 | 12,400 | 0.672 | 17,147.65 | 17,700 | 3.121 | 25,707.34 | 25,900 | 0.744 | 20,015.90 | 20,100 | 0.418 |
| 25,390.75 | 25,200 | 0.757 | 27,053.94 | 27,600 | 1.978 | 35,439.85 | 35,400 | 0.113 | 34,158.56 | 34,000 | 0.466 |
| 33,818.36 | 33,300 | 1.557 | 41,296.94 | 41,500 | 0.489 | 50,894.99 | 50,200 | 1.384 | 45,830.26 | 45,300 | 1.171 |
| 41,817.55 | 40,900 | 2.243 | 53,135.86 | 52,800 | 0.636 | 61,527.13 | 60,200 | 2.205 | 57,756.77 | 56,700 | 1.864 |
| 50,962.51 | 49,500 | 2.955 | 64,756.88 | 63,700 | 1.659 | 74,148.98 | 71,900 | 3.128 | 69,829.60 | 68,100 | 2.540 |
| 59,762.41 | 57,700 | 3.574 | 77,433.71 | 75,400 | 2.697 | 84,865.10 | 81,700 | 3.874 | 82,474.54 | 79,900 | 3.222 |
| 70,693.79 | 67,800 | 4.268 | 90,638.01 | 87,400 | 3.705 | 97,822.61 | 93,400 | 4.735 | 95,810.47 | 92,200 | 3.916 |
| 80,726.94 | 77,000 | 4.840 | 103,920.77 | 99,300 | 4.653 | 110,273.34 | 104,500 | 5.525 | 108,968.68 | 104,200 | 4.576 |
| 91,041.28 | 86,400 | 5.372 | 119,315.49 | 112,900 | 5.682 | 122,528.86 | 115,300 | 6.270 | --- | --- | --- |
| 109,381.52 | 103,000 | 6.196 | --- | --- | --- | --- | --- | --- | --- | --- | --- |

**Table S8. Experimental and calculated pressures for [MDEAH][Ac]+$H_2S$ system in various temperatures**

| [MDEAH][AC]+$H_2S$ | | | | | | | | | | |
|---|---|---|---|---|---|---|---|---|---|---|
| T=303.2 K | | | T=313.2 K | | | T=323.2 K | | | T=333.2 K | | |
| $P^{Calc.}$ (Pa) | $P^{Exp.}$ (Pa) | AAD% | $P^{Calc.}$ (Pa) | $P^{Exp.}$ (Pa) | AAD% | $P^{Calc.}$ (Pa) | $P^{Exp.}$ (Pa) | AAD% | $P^{Calc.}$ (Pa) | $P^{Exp.}$ (Pa) | AAD% |
| 9,552.99 | 9,700 | 1.516 | 13,401.55 | 13,700 | 2.178 | 17,293.25 | 17,700 | 2.298 | 12,560.04 | 12,900 | 2.635 |
| 18,188.84 | 18,400 | 1.148 | 50,130.91 | 50,500 | 0.731 | 30,673.42 | 31,200 | 1.688 | 27,335.81 | 27,900 | 2.022 |
| 28,979.87 | 29,200 | 0.754 | 61,561.03 | 61,800 | 0.387 | 44,704.95 | 45,200 | 1.095 | 42,009.20 | 42,600 | 1.387 |
| 38,017.82 | 38,200 | 0.477 | 73,853.01 | 73,900 | 0.064 | 64,677.09 | 64,900 | 0.343 | 64,183.83 | 64,500 | 0.490 |
| 47,186.70 | 47,300 | 0.240 | 85,982.34 | 85,800 | 0.213 | 74,800.00 | 74,800 | 0.000 | 77,300.00 | 77,300 | 0.000 |
| 58,500.00 | 58,500 | 0.000 | 113,595.11 | 112,800 | 0.705 | 873,42.84 | 87,000 | 0.394 | 90,830.48 | 90,400 | 0.476 |
| 71,450.49 | 71,300 | 0.211 | 127,833.80 | 126,700 | 0.895 | 100,366.44 | 99,600 | 0.770 | 104,355.93 | 103,400 | 0.924 |
| 84,001.13 | 83,700 | 0.360 | 141,048.13 | 139,600 | 1.037 | 116,679.04 | 115,300 | 1.196 | 119,863.29 | 118,200 | 1.407 |
| 96,643.64 | 96,200 | 0.461 | --- | --- | --- | --- | --- | --- | --- | --- | --- |
| 108,155.42 | 107,600 | 0.516 | --- | --- | --- | --- | --- | --- | --- | --- | --- |
| 118,534.95 | 117,900 | 0.539 | --- | --- | --- | --- | --- | --- | --- | --- | --- |

**Table S9. Experimental and calculated pressures for [MDEAH][For]+$H_2S$ system in various temperatures**

| [MDEAH][For]+$H_2S$ | | | | | | | | | | |
|---|---|---|---|---|---|---|---|---|---|---|
| T=303.2 K | | | T=313.2 K | | | T=323.2 K | | | T=333.2 K | | |
| $P^{Calc.}$ (Pa) | $P^{Exp.}$ (Pa) | AAD% | $P^{Calc.}$ (Pa) | $P^{Exp.}$ (Pa) | AAD% | $P^{Calc.}$ (Pa) | $P^{Exp.}$ (Pa) | AAD% | $P^{Calc.}$ (Pa) | $P^{Exp.}$ (Pa) | AAD% |
| 9,901.77 | 10,100 | 1.963 | 7,750.24 | 7,900 | 1.896 | 14,300.10 | 14,500 | 1.379 | 13,938.26 | 14,100 | 1.147 |
| 20,601.98 | 20,900 | 1.426 | 26,071.85 | 26,400 | 1.243 | 41,521.82 | 41,800 | 0.665 | 32,861.30 | 33,100 | 0.721 |
| 33,716.60 | 34,000 | 0.834 | 38,773.84 | 39,100 | 0.834 | 55,816.90 | 56,000 | 0.327 | 53,746.46 | 53,900 | 0.285 |
| 45,639.96 | 45,800 | 0.349 | 51,160.50 | 51,400 | 0.466 | 70,600.00 | 70,600 | 0.000 | 68,300.00 | 68,300 | 0.000 |
| 55,101.12 | 55,100 | 0.002 | 64,332.88 | 64,400 | 0.104 | 84,339.24 | 84,100 | 0.284 | 82,619.30 | 82,400 | 0.266 |
| 70,052.14 | 69,700 | 0.505 | 77,068.35 | 76,900 | 0.219 | 98,446.88 | 97,900 | 0.559 | 97,206.50 | 96,700 | 0.524 |
| 84,484.28 | 83,700 | 0.937 | 91,506.42 | 91,000 | 0.557 | 112,201.08 | 111,300 | 0.810 | 113,804.91 | 112,900 | 0.802 |
| 98,162.62 | 96,900 | 1.303 | 103,847.55 | 103,000 | 0.823 | 125,489.01 | 124,200 | 1.038 | --- | --- | --- |
| 111,793.28 | 110,000 | 1.630 | 117,472.48 | 116,200 | 1.095 | --- | --- | --- | --- | --- | --- |